Received: 3 April 2024 | Revised: 12 May 2024 | Accepted: 15 May 2024

DOI: 10.1002/bio.4794

RESEARCH ARTICLE

LUMINESCENCE WILEY
The Journal of Biological and Chemical Luminescence

Synthesis of 9-(substituted phenoxycarbonyl)-10-methylacridinium trifluoromethanesulfonates: Effects of the leaving group on chemiluminescent properties

Keith Smith[1,2] | Andy M. Holland[2] | J. Stuart Woodhead[3] | Gamal A. El-Hiti[4]

[1]School of Chemistry, Cardiff University, Main Building, Park Place, Cardiff, CF10 3AT, United Kingdom

[2]Chemistry Department, University of Wales Swansea, Singleton Park, Swansea, SA2 8PP, United Kingdom

[3]Invitron, Monmouth, United Kingdom

[4]Department of Optometry, College of Applied Medical Sciences, King Saud University, Riyadh, Saudi Arabia

Correspondence
Keith Smith, School of Chemistry, Cardiff University, Main Building, Park Place, Cardiff CF10 3AT, United Kingdom.
Email: smithk13@cardiff.ac.uk

Gamal A. El-Hiti, Department of Optometry, College of Applied Medical Sciences, King Saud University, Riyadh 11433, Saudi Arabia.
Email: gelhiti@ksu.edu.sa

Funding information
University of Wales Swansea; Cardiff University; King Saud University, Grant/Award Number: RSP2024R404; Molecular Light Technology Research Limited

Abstract

Various 9-(substituted phenoxycarbonyl)-10-methylacridinium trifluoromethanesulfonates possessing electron-withdrawing substituents have been synthesized. The effect of substituents on the stability of the acridinium esters (AEs) at various temperatures in different buffers and the chemiluminescent properties have been examined. There was little correlation between the chemiluminescent properties of AEs and the pKa values of their associated phenols, but the steric effects of the *ortho*-substituents in the phenoxy group, as well as their electron-withdrawing natures, seem to play an important role in determining the properties. In general, when two identical substituents are present in the 2- and 6-positions, the compound is significantly more stable than when only a single substituent is present, presumably because of greater steric hindrance from the second group. The exception is the 2,6-difluorophenyl ester, which is less stable than the 2-fluorophenyl ester, presumably because the fluoro group is small. Addition of a third electron-withdrawing substituent at the 4-position, where it has no steric influence, typically increases susceptibility to decomposition. The presence of a nitro group has a significant destabilizing effect on AEs. Of the AEs studied, the 4-chlorophenyl ester showed the greatest chemiluminescent yield, while the 2-iodo-6-(trifluoromethyl)phenyl ester group showed the greatest stability in low pH buffers.

KEYWORDS
9-(substituted phenoxycarbonyl)-10-methylacridinium trifluoromethanesulfonates, chemiluminescence properties, hydrolysis, stability, synthesis

1 | INTRODUCTION

Chemiluminescent materials can serve as valuable biological probes [1–3]. Acridinium esters (AEs) have proved to be particularly effective in this respect, and many differently substituted AEs have been prepared with a view to application in diagnostic technology [4–7]. The earliest report of the application of an AE involved a fluorosulfonate counter-ion [8], but subsequently, trifluoromethanesulfonate salts such as **1a** (Figure 1; $R^1 = R^2 = H$) have been favored. Many modifications of **1a** have been reported, including the use of different linker groups, leaving groups, and substituents on the nitrogen of the acridine ring [9–21] in attempts to improve its chemiluminescent

This is an open access article under the terms of the Creative Commons Attribution-NonCommercial-NoDerivs License, which permits use and distribution in any medium, provided the original work is properly cited, the use is non-commercial and no modifications or adaptations are made.
© 2024 The Author(s). *Luminescence* published by John Wiley & Sons Ltd.

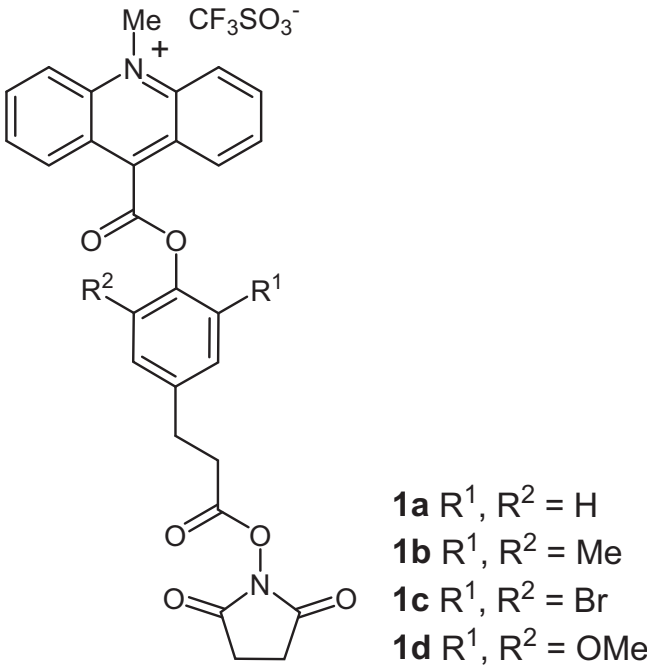

FIGURE 1 Structures of some reported acridinium esters **1**.

properties, such as quantum yield or stability. Substitution of the nitrogen of the acridine ring [11, 14–16, 18–22] can enable the luminescent unit to remain attached to the biological target after the chemiluminescent reaction. Such modifications are helpful for specific target monitoring processes [22]. Modification of the acridine ring [7, 20–25] affects the chemiluminescent properties of AEs, such as the wavelength of emission. However, the procedures for the synthesis of such AEs are often not very attractive because they may require several steps and/or involve the separation of isomeric products, which can result in poor yields and selectivity. By contrast, modification of the leaving group is relatively easy, sometimes just involving the introduction of a differently substituted phenol in the penultimate step of the synthesis. As a result, many modifications of this type have been made in order to create AEs with appropriate properties for particular purposes. For example, our group has synthesized the simple modifications of AE **1a** (i.e., **1b**, **1c**, and **1d**) shown in Figure 1 [12], among many others. Such alterations of the leaving group primarily affect the rate of the chemiluminescent reaction and of the competing non-emissive hydrolytic cleavage of the AE, which in turn affects the quantum yield of the emission.

Although many different leaving groups have been reported, very few studies allow proper comparisons of the influence of such groups. Two reviews by McCapra [26, 27] during the early development of chemiluminescent AEs referred to a relationship, for a limited range of substituted phenolic leaving groups, between the pKa of the phenol and the rate and quantum yield of the chemiluminescent reaction, but no experimental details were supplied. We have been unable to locate the substantive publication anticipated in the later one of these reviews. More recently, in 2016, a very thorough study by *Krzymiński's group* expanded the range of phenolic leaving groups studied and expanded the range of properties investigated, which included chemiluminescent reaction rates and quantum yields, different basic triggers of chemiluminescence, and effects of surfactants [17]. They were unable to confirm a universal relationship between pKa and either the rate or quantum yield of chemiluminescence. However, there was a modest relationship for rates within the series of 4-substituted phenolic systems. In addition, they briefly explored the stability of AEs in an aqueous environment at pH = 8 [17]. A high pH has a damaging effect on biological molecules, and it would be helpful to generate a chemiluminescent response at a milder level (7–9) rather than at pH = 14, at which typical AE chemiluminescence is triggered. However, at lower pH, the rate and quantum yield of the chemiluminescent reaction are lower, and emission virtually disappears at pH = 8 when the leaving group is substituted with electron-donating substituents [17]. In practice, it becomes necessary to utilize a leaving group with electron-withdrawing substituents in order to operate at such lower pH values [22]. Of course, changing the nature of the leaving group will also affect the rate of the hydrolysis of the ester group, which leads to a non-emissive pathway and a concomitant effect on the overall efficiency of the chemiluminescence. Furthermore, for many applications, the probe molecule must be incubated with the target analyte for some time prior to initiation of the chemiluminescence, and any hydrolysis of the ester group during this period will inevitably degrade the efficiency of emission. Therefore, it is important to understand the effects of different electron-withdrawing groups on both the initial chemiluminescence efficiency and the residual chemiluminescence after incubation at various pH values. In the current study, we examine how these chemiluminescence properties of AEs are affected by a range of electron-withdrawing substituents in a series of 9-(substituted phenoxycarbonyl)-10-methylacridinium trifluoromethanesulfonates **2–25** (Figure 2; Table 1). The AEs chosen are substituted in the 2, 4, and/or 6-positions because 4-substituted compounds will be influenced primarily by electronic effects, whereas 2 and 6-substituted compounds will also exhibit steric effects. Because simple 4-substituted compounds have had extensive study previously [17, 26, 27], all of the examples in the current study, except for the unsubstituted example (Compound **2**), have at least one *ortho*-substituent.

2 | EXPERIMENTAL

2.1 | General

The general experimental details, including details of spectroscopic instrumentation, along with the syntheses of precursors **28a–x** (Scheme 1), are given in the Supporting information (Scheme S1 and Table S1). Only data for the final AE products are recorded here. In the ^{13}C nuclear magnetic resonance (CNMR) spectra of the AEs recorded below, the signal due to the trifluoromethanesulfonate anion is not recorded because it often could not be reliably detected as it was weak and coupled to three fluorine nuclei. High-resolution mass spectrometry was used to measure accurately the mass-charge ratio

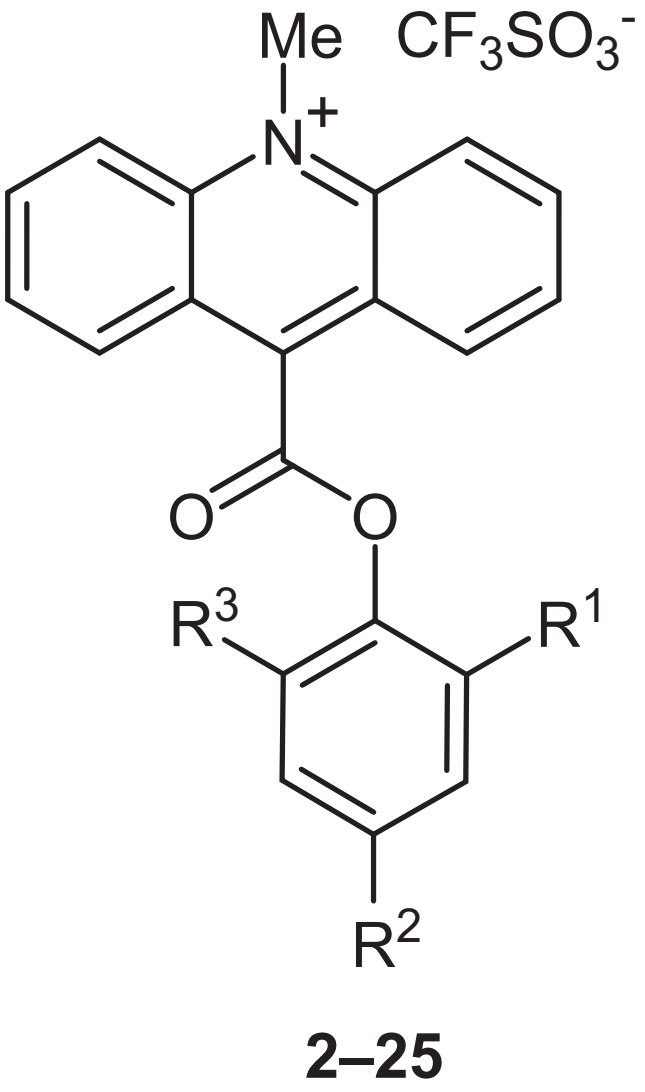

FIGURE 2 Structures of target acridinium esters **2–25**.

for one isotopic example of the cation part of each AE molecule to confirm its elemental composition.

2.2 | General procedure for the synthesis of 9-(substituted phenoxycarbonyl)-10-methylacridinium trifluoromethanesulfonates 2–25

Mixtures of the appropriately substituted-phenyl acridine-9-carboxylate **28a–x** (0.207–0.939 mmol), dry dichloromethane (DCM, 5 mL), and excess CF_3SO_3Me (approximately 7-mole equivalents) were stirred under N_2 for 3 h at 20°C. The solids obtained were removed by filtration, washed with Et_2O, and dried to give the corresponding AEs **2–25** as bright yellow materials in 33%–98% yields (Table 1). Some of the compounds have been reported previously. The references to those compounds are listed in Table 1. Nevertheless, the known and new compounds were all synthesized in the course of this work in order to provide samples for study.

2.2.1 | 9-(Phenoxycarbonyl)-10-methylacridinium trifluoromethanesulfonate (**2**) [28, 29]

^{1}H NMR (DMSO-d_6) δ: 8.96 (d, 9.3 Hz, 2H), 8.65 (app. d, 8.6 Hz, 2H), 8.57 (ddd, 9.3, 6.8, 1.3 Hz, 2H), 8.19 (dd, 8.4, 6.8 Hz, 2H), 7.78 (app. t, 7.8 Hz, 2H), 7.65 (d, 8.4 Hz, 2H), 7.51 (t, 7.4 Hz, 1H), 4.96 (s, 3H). ^{13}C NMR (DMSO-d_6) δ: 163.6, 149.6, 146.8, 142.0, 139.3, 130.2, 129.9, 127.6, 125.3, 122.3, 121.9, 120.0, 39.9.

2.2.2 | 9-(2-Fluorophenoxycarbonyl)-10-methylacridinium trifluoromethanesulfonate (**3**) [17]

IR υ_{max} (KBr): 1774, 1615, 1502, 1260 cm^{-1}. ^{1}H NMR ($CDCl_3$) δ: 8.98 (d, 9.4 Hz, 2H), 8.55–8.59 (m, 4H), 8.22 (dd, 8.6, 6.8 Hz, 2H), 7.97 (app. td, 7.9, 1.5 Hz, 1H), 7.65 (ddd, 10.8, 8.9, 1.4 Hz, 1H), 7.56–7.60 (m, 1H), 7.49 (app. t, 7.1 Hz, 1H), 4.98 (s, 3H). ^{13}C NMR ($CDCl_3$) δ: 162.6, 154.4, 152.0, 146.0, 142.0, 139.3, 130.0, 129.5, 127.1, 125.9, 124.4, 122.5, 120.1, 117.4, 40.0. ES$^+$–HRMS: calculated: 332.1087 ($C_{21}H_{15}FNO_2$); found: 332.1086.

2.2.3 | 9-(2-Chlorophenoxycarbonyl)-10-methylacridinium trifluoromethanesulfonate (**4**) [17]

IR υ_{max} (KBr): 1759, 1475, 1276, 1263 cm^{-1}. ^{1}H NMR (DMSO-d_6) δ: 8.98 (d, 9.3 Hz, 2H), 8.68 (dd, 8.4, 1.0 Hz, 2H), 8.58 (ddd, 9.3, 6.9, 1.0 Hz, 2H), 8.23 (dd, 8.4, 6.9 Hz, 2H), 8.09 (dd, 8.1, 1.5 Hz, 1H), 7.83 (dd, 8.0, 1.5 Hz, 1H), 7.67 (app. td, 7.8. 1.5 Hz, 1H), 7.56 (app. td, 7.7, 1.5 Hz, 1H), 4.98 (s, 3H). ^{13}C NMR (DMSO-d_6) δ: 162.8, 145.9, 145.3, 142.0, 139.3, 130.9, 130.0, 129.4, 129.2, 127.3, 125.4, 124.6, 122.5, 120.1, 40.0. ES$^+$–HRMS: calculated: 348.0791 ($C_{21}H_{15}{}^{35}ClNO_2$); found: 348.0792.

2.2.4 | 9-(2-Bromophenoxycarbonyl)-10-methylacridinium trifluoromethanesulfonate (**5**) [17]

IR υ_{max} (KBr): 1757, 1274, 1269, 1204 cm^{-1}. ^{1}H NMR (DMSO-d_6) δ: 8.98 (d, 9.3 Hz, 2H), 8.73 (app. D, 8.5 Hz, 2H), 8.58 (ddd, 9.3, 6.9, 1.3 Hz, 2H), 8.23 (dd, 8.5, 6.9 Hz, 2H), 8.08 (dd, 8.1, 1.4 Hz, 1H), 7.94 (dd, 8.0, 1.4 Hz, 1H), 7.70 (app. td, 7.8, 1.4 Hz, 1H) 7.48 (app. td, 7.7, 1.4 Hz, 1H), 4.98 (s, 3H). ^{13}C NMR (DMSO-d_6) δ: 162.9, 146.7, 145.9, 142.0, 139.3, 133.9, 129.9, 129.8, 129.6, 127.4, 124.6, 122.5, 120.1, 114.9, 40.0. ES$^+$–HRMS: calculated: 392.0286 ($C_{21}H_{15}{}^{79}BrNO_2$); found: 392.0291.

2.2.5 | 9-(2-Iodophenoxycarbonyl)-10-methylacridinium trifluoromethanesulfonate (**6**) [17]

IR υ_{max} (KBr): 1755, 1264, 1202 cm^{-1}. ^{1}H NMR (DMSO-d_6) δ: 8.98 (d, 9.3 Hz, 2H), 8.79 (d, 8.5 Hz, 2H), 8.59 (dd, 9.3, 6.8 Hz, 2H), 8.21 (dd,

TABLE 1 Synthesis of acridinium esters (AEs) **2–25** according to Scheme 1.

Precursor 28	R^1	R^2	R^3	Product AE	m.p. (°C)	Yield (%)	Reference
28a	H	H	H	**2**	222	86	[28, 29]
28b	F	H	H	**3**	113	90	[17]
28c	Cl	H	H	**4**	222	86	[17]
28d	Br	H	H	**5**	230	48	[17]
28e	I	H	H	**6**	227	86	[17]
28f	NO_2	H	H	**7**	232	86	[17]
28g	CF_3	H	H	**8**	235	34	[17]
28h	CN	H	H	**9**	237	86	
28i	MeCO	H	H	**10**	240	92	
28j	F	H	F	**11**	243	59	[17]
28k	Cl	H	Cl	**12**	252	70	[17]
28l	Br	H	Br	**13**	200	80	[17]
28m	CF_3	H	CF_3	**14**	202	38	
28n	I	H	CF_3	**15**	202	74	
28o	C_6H_5CO	Cl	H	**16**	235	69	
28p	4-ClC_6H_4CO	F	H	**17**	230	33	
28q	F	F	F	**18**	240	61	
28r	Cl	Cl	Cl	**19**	255	98	
28s	Br	Br	Br	**20**	268	51	
28t	Cl	Cl	NO_2	**21**	224	61	
28u	F	Br	NO_2	**22**	229	61	
28v	Br	NO_2	Br	**23**	233	48	
28w	MeCO	Cl	Cl	**24**	260	56	
28x	MeCO	Br	Br	**25**	260	80	

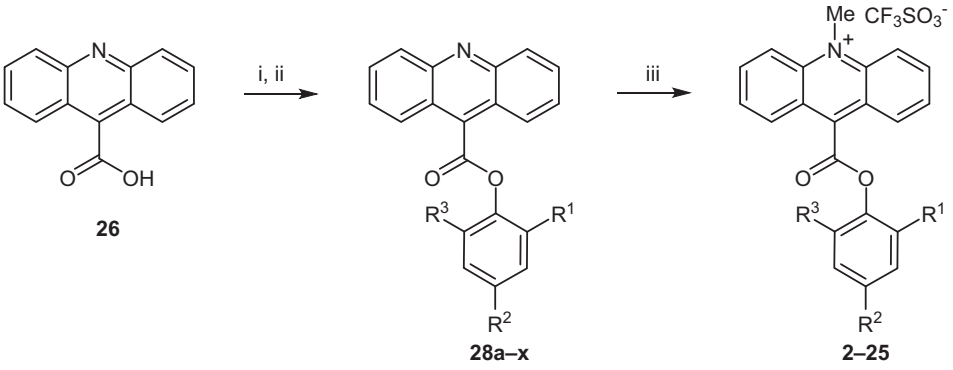

26 **28a–x** **2–25**

SCHEME 1 Synthesis of acridinium esters (AEs) **2–25**.

Reagents: i: $SOCl_2$, ii: pyridine, substituted phenols **27a–x**, iii: CF_3SO_3Me, DCM

8.5, 6.8 Hz, 2H), 8.09 (dd, 7.9, 1.4 Hz, 1H), 8.05 (dd, 8.2, 1.3 Hz, 1H), 7.70 (app. td, 7.8, 1.4 Hz, 1H), 7.30 (app. td, 7.6, 1.3 Hz, 1H), 4.98 (s, 3H). ^{13}C NMR (DMSO-d_6) δ: 163.0, 150.1, 146.0, 142.0, 140.0, 139.3, 130.3, 129.8, 129.6, 127.7, 123.8, 122.5, 120.1, 90.4, 40.0. ES^+–HRMS: calculated: 440.0148 ($C_{21}H_{15}INO_2$); found: 440.0150.

2.2.6 | 9-(2-Nitrophenoxycarbonyl)-10-methylacridinium trifluoromethanesulfonate (**7**) [17]

IR υ_{max} (KBr): 2918, 2850, 1764, 1601, 1538, 1524, 1350, 1264 cm^{-1}. ^1H NMR (DMSO-d_6) δ: 8.98 (d, 9.3 Hz, 2H), 8.70 (app. d, 8.5 Hz, 2H),

8.58 (ddd, 9.3, 6.9, 1.2 Hz, 2H), 8.37 (dd, 8.2, 1.5 Hz, 1H), 8.27 (dd, 8.2, 1.1 Hz, 1H), 8.22 (app. dd, 8.5, 6.9 Hz, 2H), 8.09 (app. dd, 7.9, 1.5 Hz, 1H), 7.80 (app. dd, 7.9, 1.1 Hz, 1H), 4.99 (s, 3H). ^{13}C NMR (DMSO-d_6) δ: 162.6, 145.0, 142.6, 142.0, 141.4, 139.2, 136.1, 129.8, 129.1, 127.3, 126.4, 125.7, 122.7, 120.1, 40.1. ES$^+$–HRMS: calculated: 359.1032 ($C_{21}H_{15}N_2O_4$); found: 359.1038.

2.2.7 | 9-(2-Trifluoromethylphenoxycarbonyl)-10-methylacridinium trifluoromethanesulfonate (**8**) [17]

IR υ_{max} (KBr): 1773, 1614, 1325, 1268 cm^{-1}. ^{1}HNMR (DMSO-d_6) δ: 8.99 (d, 9.5 Hz, 2H), 8.56–8.60 (m, 4H), 8.37 (d, 8.2 Hz, 1H), 8.21 (app. t, 7.7 Hz, 2H), 8.01–8.05 (m, 2H), 7.74 (app. t, 7.7 Hz, 1H), 4.98 (s, 3H). ^{13}CNMR (DMSO-d_6) δ: 162.8, 146.3, 145.3, 142.1, 139.3, 134.9, 129.9, 128.4, 127.65, 127.60, 125.0, 122.5, 121.1, 120.2, 95.7, 40.1. ES$^+$–HRMS: calculated: 382.1055 ($C_{22}H_{15}F_3NO_2$); found: 382.1054.

2.2.8 | 9-(2-Cyanophenoxycarbonyl)-10-methylacridinium trifluoromethanesulfonate (**9**)

IR υ_{max} (KBr): 1754, 1608, 1201 cm^{-1}. ^{1}HNMR (DMSO-d_6) δ: 8.99 (app. d, 9.3 Hz, 2H), 8.70 (dd, 8.6, 0.7 Hz, 2H), 8.57 (ddd, 9.3, 6.8, 1.3 Hz, 2H), 8.23 (d, 8.3 Hz, 1H), 8.14–8.19 (m, 3H), 8.04 (app. td, 8.0, 1.5 Hz, 1H), 7.71 (app. td, 7.6, 0.8 Hz, 1H), 4.99 (s, 3H). ^{13}CNMR (DMSO) δ: 162.7, 150.3, 146.0, 142.0, 139.3, 135.7, 134.4, 129.8, 128.6, 127.3, 123.9, 122.5, 120.1, 115.4, 105.7, 40.0. ES$^+$–HRMS: calculated: 339.1134 ($C_{22}H_{15}N_2O_2$); found 339.1131.

2.2.9 | 9-(2-Acetylphenoxycarbonyl)-10-methylacridinium trifluoromethanesulfonate (**10**)

IR υ_{max} (KBr): 1753, 1691, 1608, 1270 cm^{-1}. ^{1}HNMR (DMSO-d_6) δ: 8.94 (d, 9.3 Hz, 2H), 8.82 (d, 8.4 Hz, 2H), 8.55 (app. t, 7.5 Hz, 2H), 8.18–8.22 (m, 3H), 7.87–7.91 (m, 2H), 7.65 (app. t, 7.1 Hz, 1H), 4.97 (s, 3H), 2.65 (s, 3H). ^{13}CNMR (DMSO) δ: 198.2, 163.0, 146.8, 146.4, 142.0, 139.2, 134.2, 131.9, 130.7, 129.5, 128.0, 125.5, 124.1, 122.7, 119.8, 39.8, 29.2. ES$^+$–HRMS: calculated: 356.1287 ($C_{23}H_{18}NO_3$); found: 356.1291.

2.2.10 | 9-(2,6-Difluorophenoxycarbonyl)-10-methylacridinium trifluoromethanesulfonate (**11**) [17]

IR υ_{max} (KBr): 1776, 1611, 1496, 1480, 1264 cm^{-1}. ^{1}H NMR (DMSO-d_6) δ: 9.01 (d, 9.5 Hz, 2H), 8.59 (ddd, 9.5, 6.8, 1.2 Hz, 2H), 8.42 (app. d, 8.6 Hz, 2H), 8.27 (dd, 8.6, 6.8 Hz, 2H), 7.62–7.66 (m, 1H), 7.54–7.60 (m, 2H), 5.00 (s, 3H). ^{13}C NMR (DMSO-d_6) δ: 161.9, 155.4, 153.0, 145.0, 142.0, 139.4, 130.3, 129.5, 113.5, 126.4, 126.0, 122.5, 120.3, 40.1 (the extra lines are due to C–F coupling). ES$^+$–HRMS: calculated mass: 350.0993 ($C_{21}H_{14}F_2NO_2$); found: 350.0994.

2.2.11 | 9-(2,6-Dichlorophenoxycarbonyl)-10-methylacridinium trifluoromethanesulfonate (**12**) [17]

IR υ_{max} (KBr): 1767, 1446, 1273, 1160 cm^{-1}. ^{1}H NMR (DMSO-d_6) δ: 8.99 (d, 9.3 Hz, 2H), 8.77 (d, 8.6 Hz, 2H), 8.58 (app. t, 8.2 Hz, 2H), 8.25 (app. t, 7.7 Hz, 2H), 7.82 (d, 8.2 Hz, 2H), 7.58 (t, 8.2 Hz, 1H), 5.00 (s, 3H). ^{13}C NMR (DMSO-d_6) δ: 161.6, 145.1, 142.1, 142.0, 139.3, 129.9, 127.2, 130.0, 127.7, 127.1, 122.8, 120.2, 40.2. ES$^+$–HRMS: calculated: 382.0402 ($C_{21}H_{14}{}^{35}Cl_2NO_2$); found: 382.0405.

2.2.12 | 9-(2,6-Dibromophenoxycarbonyl)-10-methylacridinium trifluoromethanesulfonate (**13**) [17]

IR υ_{max} (KBr): 1763, 1272, 1205, 1154 cm^{-1}. ^{1}H NMR ($CDCl_3$) δ: 9.00 (d, 9.3 Hz, 2H), 8.95 (d, 8.6 Hz, 2H), 8.59 (app. t, 7.9 Hz, 2H), 8.25 (dd, 8.6, 6.9 Hz, 2H), 8.00 (d, 8.4 Hz, 2H), 7.43 (t, 8.4 Hz, 1H), 5.00 (s, 3H). ^{13}C NMR ($CDCl_3$) δ: 161.8, 156.7, 144.7, 142.0, 139.2, 133.7, 130.9, 129.8, 127.5, 122.9, 120.2, 116.9, 39.97. ES$^+$–HRMS: calculated: 469.9391 ($C_{21}H_{14}{}^{79}Br_2NO_2$); found: 469.9394.

2.2.13 | 9-(2,6-Bis(trifluoromethyl) phenoxycarbonyl)-10-methylacridinium trifluoromethanesulfonate (**14**)

IR υ_{max} (KBr): 1768, 1610, 1260, 1201 cm^{-1}. ^{1}H NMR (DMSO-d_6) δ: 9.00 (d, 9.3 Hz, 2H), 8.59 (d, 8.7 Hz. 2H), 8.55 (dd, 9.3,6.8 Hz, 2H), 8.17 (dd, 8.7, 6.8 Hz, 2H), 7.88–7.92 (m, 2H), 7.62 (t, 7.5 Hz, 1H), 5.14 (s, 3H). ^{13}CNMR (DMSO-d_6) δ: 163.6, 147.8, 147.7, 143.4, 142.0, 140.5, 130.7, 128.9, 128.4, 125.5, 123.9, 120.6, 97.1, 40.6. ES$^+$–HRMS: calculated mass: 450.0929 ($C_{23}H_{14}F_6NO_2$); found: 450.0925.

2.2.14 | 9-(2-Trifluoromethyl-6-iodophenoxycarbonyl)-10-methylacridinium trifluoromethanesulfonate (**15**)

IR υ_{max} (KBr): 1762, 1266, 1270, 1204 cm^{-1}. ^{1}H NMR (DMSO-d_6) δ: 8.87–9.03 (m, 3H), 8.76–8.82 (m, 3H), 8.22 (dd, 8.8, 6.9 Hz, 2H), 8.04 (dd, 8.8, 6.9 Hz, 2H), 7.77 (app. t, 7.6 Hz, 1H), 4.98 (s, 3H). ^{13}C NMR (DMSO-d_6) δ: 162.8, 147.1, 145.3, 143.7, 142.1, 139.3, 139.0, 134.9, 130.1, 130.0, 128.4, 127.0, 125.0, 122.4, 123.3, 120.2, 90.0, 40.0 (the

extra visible lines are due to C–F coupling). ES^+–HRMS: calculated: 508.0021 ($C_{22}H_{14}F_3INO_2$); found: 508.0027.

2.2.15 | 9-(2-Benzoyl-4-chlorophenoxycarbonyl)-10-methylacridinium trifluoromethanesulfonate (**16**)

IR υ_{max} (KBr): 1758, 1668, 1610, 1281, 1263 cm^{-1}. ^1H NMR (DMSO-d_6) δ: 8.90 (d, 9.4 Hz, 2H), 8.51 (ddd, 9.6, 6.7, 1.2 Hz, 2H), 8.36 (dd, 8.6, 1.2 Hz, 2H), 8.21 (d, 8.6 Hz, 1H), 8.08 (dd, 8.6, 6.7 Hz, 2H), 7.99 (dd, 8.6, 2.6 Hz, 1H), 7.87 (d, 2.6 Hz, 1H), 7.83 (d, 7.8 Hz, 2H), 7.73 (t, 7.8 Hz, 1H), 7.57 (app. t, 7.8 Hz, 2H), 4.91 (s, 3H). ^{13}C NMR (DMSO-d_6) δ: 192.5, 163.0, 145.5, 145.3, 141.9, 139.1, 135.4, 134.8, 133.4, 132.3, 132.0, 130.1, 129.6, 129.4, 129.2, 127.1, 125.8, 122.4, 120.0, 39.9. ES^+–HRMS: calculated: 452.1053 ($C_{28}H_{19}{}^{35}ClNO_3$); found: 452.1057.

2.2.16 | 9-(2-(4-Chlorobenzoyl)-4-fluorophenoxycarbonyl)-10-methylacridinium trifluoromethanesulfonate (**17**)

IR υ_{max} (KBr): 1753, 1663, 1585, 1265, 1227 cm^{-1}. ^1H NMR (DMSO-d_6) δ: 8.91 (d, 9.4 Hz, 2H), 8.53 (dd, 9.4, 6.8 Hz, 2H), 8.42 (d, 8.6 Hz, 2H), 8.22 (dd, 9.0, 4.4 Hz, 1H), 8.11 (dd, 8.6, 6.8 Hz, 2H), 7.85 (d, 8.6 Hz, 2H), 7.77–7.82 (m, 1H), 7.73 (dd, 8.6, 3.1 Hz, 1H), 7.62 (d, 8.6 Hz, 2H), 4.91 (s, 3H). ^{13}C NMR (DMSO-d_6) δ: 191.6, 163.2, 158.6, 145.6, 142.7, 141.9, 139.7, 139.2, 134.1, 132.7, 131.9, 129.6, 129.3, 127.2, 126.1, 122.4, 120.0, 119.5, 117.0, 40.0. ES^+–HRMS: calculated: 470.0959 ($C_{28}H_{18}{}^{35}ClFNO_3$); found: 470.0968.

2.2.17 | 9-(2,4,6-Trifluorophenoxycarbonyl)-10-methylacridinium trifluoromethanesulfonate (**18**)

IR υ_{max} (KBr): 1772, 1610, 1557, 1262 cm^{-1}. ^1H NMR (DMSO-d_6) δ: 9.0 (d, 9.4 Hz, 2H), 8.91 (dd, 8.6, 1.1 Hz, 2H), 8.57 (ddd, 9.4, 6.8, 1.1 Hz, 2H), 8.24–8.28 (m, 4H), 4.99 (s, 3H). ^{13}C NMR (DMSO-d_6) δ: 161.2, 150.5, 147.8, 144.6, 141.8, 139.2, 135.5, 129.7, 127.4, 122.8, 120.0, 117.9, 40.2. ES^+–HRMS: calculated: 368.0898 ($C_{21}H_{13}F_3NO_2$); found: 368.0902.

2.2.18 | 9-(2,4,6-Trichlorophenoxycarbonyl)-10-methylacridinium trifluoromethanesulfonate (**19**)

IR υ_{max} (KBr): 1749, 1474, 1444, 1205 cm^{-1}. ^1H NMR (DMSO-d_6) δ: 9.0 (d, 9.4 Hz, 2H), 8.72 (d, 8.3 Hz, 2H), 8.59 (app. t, 8.0 Hz, 2H), 8.27 (dd, 8.3, 7.0 Hz, 2H), 7.75 (s, 2H), 4.99 (s, 3H). ^{13}C NMR (DMSO-d_6) δ: 161.7, 144.6, 142.0, 141.3, 139.3, 133.4, 130.1, 129.8, 128.6, 126.9, 122.8, 120.2, 40.2. ES^+–HRMS: calculated: 416.0012 ($C_{21}H_{13}{}^{35}Cl_3NO_2$); found: 416.0012.

2.2.19 | 9-(2,4,6-Tribromophenoxycarbonyl)-10-methylacridinium trifluoromethanesulfonate (**20**)

IR υ_{max} (KB): 1748, 1280, 1201 cm^{-1}. ^1H NMR (DMSO-d_6) δ: 9.01 (d, 9.3 Hz, 2H), 8.59 (dd, 9.3, 6.8 Hz, 2H), 8.40 (d, 8.6 Hz, 2H), 8.26 (dd, 8.6, 6.8 Hz, 2H), 7.75 (s, 2H), 4.99 (s, 3H). ^{13}C NMR (DMSO-d_6) δ: 161.8, 155.5, 153.2, 144.8, 142.0, 139.4, 130.3 (two overlapping signals), 102.5, 126.4, 122.5, 120.3, 40.0. ES^+–HRMS: calculated: 547.8496 ($C_{21}H_{13}{}^{79}Br_3NO_2$); found: 547.8491.

2.2.20 | 9-(2,4-Dichloro-6-nitrophenoxycarbonyl)-10-methylacridinium trifluoromethanesulfonate (**21**)

IR υ_{max} (KBr): 1770, 1556, 1268 cm^{-1}. ^1H NMR (DMSO-d_6) δ: 8.86 (d, 9.3 Hz, 2H), 8.49 (app. t, 9.0 Hz, 2H), 8.41 (d, 8.6 Hz, 2H), 8.10 (app. t, 8.0 Hz, 2H), 8.02 (d, 2.0 Hz, 1H), 8.00 (d, 2.0 Hz, 1H), 5.00 (s, 3H). ^{13}C NMR (DMSO-d_6) δ: 161.2, 143.3, 143.7, 142.0, 141.9, 139.2, 138.9, 137.8, 129.9, 128.9, 127.1, 123.0, 120.2, 119.7, 40.4. ES^+–HRMS: calculated: 427.0252 ($C_{21}H_{13}{}^{35}Cl_2N_2O_4$); found: 427.0256.

2.2.21 | 9-(4-Bromo-2-fluoro-6-nitrophenoxycarbonyl)-10-methylacridinium trifluoromethanesulfonate (**22**)

IR υ_{max} (KBr): 1783, 1549, 1278, 1260 cm^{-1}. ^1H NMR (DMSO-d_6) δ: 9.07 (d, 9.4 Hz, 2H), 8.70 (d, 8.5 Hz, 2H), 8.64 (dd, 9.4, 7.0 Hz, 2H), 8.40 (app. t, 2.2 Hz, 1H), 8.35 (dd, 9.4, 2.2 Hz, 1H), 8.28 (dd, 8.5, 7.0 Hz, 2H), 5.00 (s, 3H). ^{13}C NMR (DMSO-d_6) δ: 161.2, 155.4, 152.8, 144.1, 142.8, 142.0, 139.3, 130.0, 128.8, 126.7, 125.1, 122.8, 121.5, 120.3, 40.2. ES^+–HRMS: calculated: 455.0043 ($C_{21}H_{13}{}^{79}BrFN_2O_4$); found: 455.0041.

2.2.22 | 9-(2,6-Dibromo-4-nitrophenoxycarbonyl)-10-methylacridinium trifluoromethanesulfonate (**23**)

IR υ_{max} (KBr): 1768, 1611, 1532, 1347, 1267 cm^{-1}. ^1H NMR (DMSO-d_6) δ: 9.01 (d, 9.4 Hz, 2H), 8.94 (d, 8.6 Hz, 2H), 8.83 (s, 2H), 8.60 (dd, 9.4, 6.8 Hz, 2H), 8.26 (dd, 8.6, 6.8 Hz, 2H), 5.01 (s, 3H). ^{13}C NMR (DMSO-d_6) δ: 161.1, 149.6, 147.1, 144.0, 142.0, 139.3, 130.0, 127.4, 122.9, 120.2, 118.0, 40.4 (one peak not seen due to overlap or weak signal). ES^+–HRMS: calculated: 514.9242 ($C_{21}H_{13}{}^{79}Br_2N_2O_4$); found: 514.9239.

2.2.23 | 9-(2-Acetyl-4,6-dichlorophenoxycarbonyl)-10-methylacridinium trifluoromethanesulfonate (**24**)

IR υ_{max} (KBr): 1755, 1707, 1270 cm^{-1}. ^1H NMR (DMSO-d_6) δ: 8.97 (d, 9.4 Hz, 2H), 8.85 (d, 8.6 Hz, 2H), 8.56 (app. t, 8.6 Hz, 2H), 8.32 (d, 2.5 Hz, 1H), 8.29 (d, 2.5 Hz, 1H), 8.21 (dd, 8.6, 6.7 Hz, 2H), 4.99

(s, 3H), 2.68 (s, 3H). ^{13}C NMR (DMSO-d_6) δ: 197.7, 161.9, 144.8, 142.0, 141.8, 139.1, 133.9, 133.6, 132.9, 129.8, 129.5, 128.8, 127.7, 123.0, 120.0, 40.3, 29.5. ES$^+$–HRMS: calculated: 424.0507 ($C_{23}H_{16}{}^{35}Cl_2NO_3$); found: 424.0515.

2.2.24 | 9-(2-Acetyl-4,6-dibromophenoxycarbonyl)-10-methylacridinium trifluoromethanesulfonate (**25**)

IR υ_{max} (KBr): 1753, 1705, 1268 cm^{-1}. ^{1}H NMR (DMSO-d_6) δ: 8.97 (d, 9.4 Hz, 2H), 8.89 (d, 8.6 Hz, 2H), 8.56 (app. t, 7.9 Hz, 2H), 8.49 (d, 2.3 Hz, 1H), 8.42 (d, 2.3 Hz, 1H), 8.20 (app. t, 8.4 Hz, 2H), 4.99 (s, 3H), 2.68 (s, 3H). ^{13}C NMR (DMSO-d_6) δ: 197.8, 161.8, 145.5, 144.8, 142.0, 139.2, 139.1, 134.2, 132.8, 129.4, 127.9, 123.1, 121.1, 120.0, 118.8, 40.3, 29.5. ES$^+$–HRMS: calculated: 511.9497 ($C_{23}H_{16}{}^{79}Br_2NO_3$); found: 511.9504.

2.3 | Chemiluminescence measurements

2.3.1 | Kinetics measurements

During kinetic mode, the chemiluminescence of the synthesized AEs was tested using standard reagents provided by Molecular Light Technology Research Ltd. The chemiluminescence measurement period was manually controlled, with the maximum intensity set at 88 relative light units (RLUs). The output was recorded in RLU at 1/10th of the period of significant chemiluminescent output. The results are presented graphically, with trend lines generated using Excel.

2.3.2 | Measurement of chemiluminescent efficiency and hydrolytic stability

The hydrolytic stabilities of AEs were investigated using a reported procedure [12]. AEs were dissolved in acetonitrile (MeCN) and then diluted to a concentration of 1.00×10^{-4} mg/mL using MeCN [12]. After diluting the substance multiple times, it was mixed with pH 6.0, 7.0, or 8.0 phosphate buffers to produce solutions with a concentration of 1.00 nmol/L at each pH level. The solutions were tested at 4, 25, and 37°C. The luminescence measurement period was fixed at 15 s, and the results are illustrated graphically using Excel.

2.3.3 | Caution over the accuracy of chemiluminescence measurements

This study required a number of different types of experiments, some of which had to be monitored over several weeks, for 24 compounds at up to 6 pH values and at three different temperatures, so it was impractical to carry out the individual experiments more than once. Consequently, individual results may be subject to a significant margin of error, the size of which is not known. Therefore, only the trends, rather than the actual values, are important.

3 | RESULTS AND DISCUSSION

3.1 | Syntheses

The route used for syntheses of AEs **2–25**, involving esterification of acridine-9-carboxylic acid with the appropriate phenol followed by methylation on the nitrogen atom, is illustrated in Scheme 1. The yields and the melting points of the AEs are summarized in Table 1. The chemical structures were confirmed using various spectroscopic techniques, as reported in Section 2.2.

3.2 | Chemiluminescent properties

The pKa values of the substituted phenols **27a–x** (Scheme 1) vary from 4.0 to 10.2 based on literature reports [30, 31]. The highest pKa value is for 2-acetylphenol and the lowest for 4-bromo-2-fluoro-6-nitrophenol. It is worth noting that pKa values of substituted phenols capable of forming internal hydrogen bonds tend to be higher than would be expected based purely on the electronic effects of the substituents. Hence, their pKa values are not as helpful as those of other phenols in indicating the ease of displacement of the anion in the chemiluminescent reaction of their AEs. The influence of the different phenoxide leaving groups on the stability of esters in solution, the kinetics of the chemiluminescent reaction, and the total light emission from the chemiluminescent reaction was examined.

3.2.1 | Chemiluminescent characteristics

The influence of the leaving group on the chemiluminescent characteristics of AEs **2–25** was studied at pH ranges from 7 to 12. A luminometer (Ciba-Corning Magic Lite Analyzer) was used to monitor chemiluminescence. A 10 μL sample solution was placed into a tube and inserted into the luminometer. The machine automatically added the required reagents to initiate light emission. The resulting kinetics curve (intensity of light output versus time) was generated, followed by the total light output over 15 s, expressed in RLUs [19]. To initiate chemiluminescence, an acidic solution of hydrogen peroxide was injected into an aqueous solution of the AE, followed by injection of a buffer solution of the appropriate pH, and the light emission was tracked using the luminometer. Initially, kinetic plots were recorded at each pH value for each AE, all normalized to the same maximum emission intensity. At any particular pH, the plots for all of the AEs were very similar, reaching maximum emission intensity at roughly the same time and showing similar trends as the light intensity diminished. This was particularly true at the higher pH values (9–12). However, at the lower pH values, the differences were more noticeable, with a few

AEs displaying a significantly slower diminution of light intensity than the majority.

Nevertheless, the level of similarity of the plots for all of the AEs at all pH values was such that the average characteristics of all of the AEs at any given pH value was more informative than the differences between the AEs. Three average parameters were calculated for each pH value: the time taken to reach maximum emission intensity (T_{max}), the time at which the emission intensity had fallen to 25% of its maximum intensity (T_{25}), and the time needed to collect most of the light emitted (T_c). The last parameter is most meaningful for the higher pHs (9–12) because, at pH 8, the slowest reacting AE still showed 25% of the maximum emission level after 8 s. At pH 7, the slowest reacting AE still showed 50% of maximum emission after 30 s. Therefore, for these low pH values, the measurement period was set at 30 s, and the average T_c values, particularly for the case of pH 7, are subject to a larger margin of error than for the higher pH values. Nevertheless, the data are sufficient to show the differences between the emission profiles at different pH values.

The three average parameters are plotted in Figure 3. As the results show, all three parameters drop in value as the pH increases. At pH 12, the reactions were very rapid, so the average time for the emission to reach maximum intensity was only 0.2 s, and all light could be captured within 1 s. However, at pH 7, the average time for emission to reach maximum intensity was 3 s, the average time for the intensity to drop to 25% of its maximum was around 17 s, and even after 30 s, not all of the light emitted could be captured.

In order to investigate the effect of the leaving groups in more detail, the AEs **2–25** were organized into three groups based on their substituents. The first group included eight AEs with monosubstituted phenoxy groups (i.e., AEs **3–10**) along with unsubstituted AE **2** for comparison. The pKa values of the phenols associated with AEs **2–10** are shown in Figure 4 [30, 31].

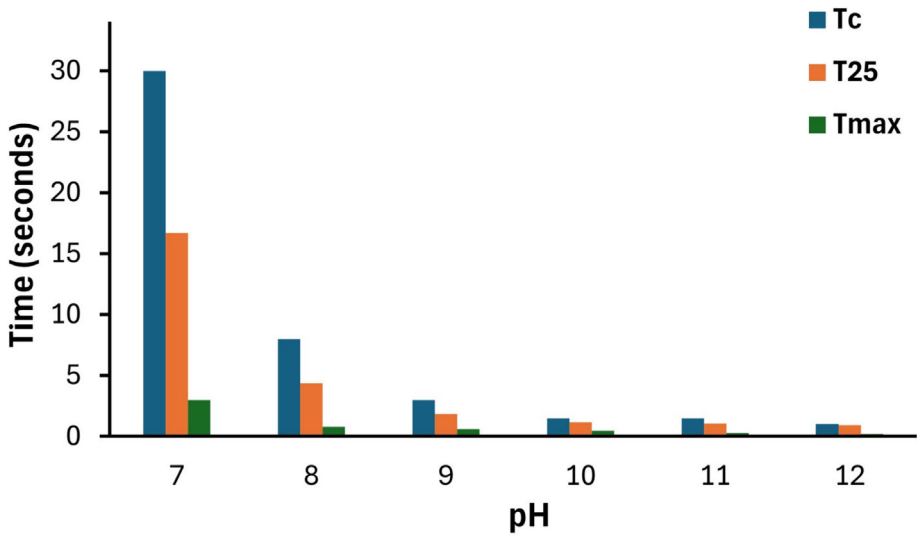

FIGURE 3 Average times for light emission from acridinium esters (AEs). Tc is the time needed to collect most of the emitted light from AEs, T_{25} is the average time taken for light intensity to drop to 25% of the maximum intensity, and T_{max} is the average time taken to reach maximum light intensity.

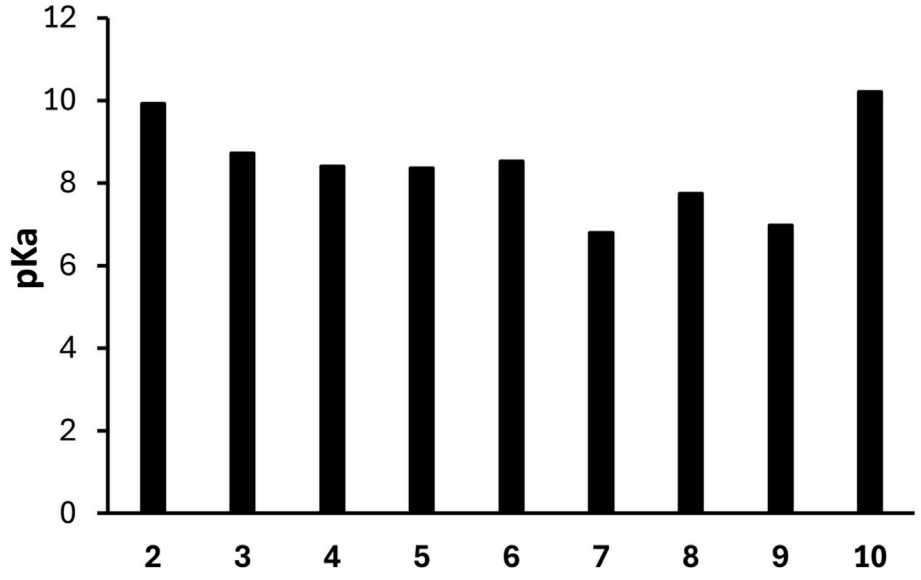

FIGURE 4 The pKa of the phenols associated with the ester groups of acridinium esters (AEs) **2–10**.

The effects of pH on the maximum chemiluminescent emission intensity (in RLUs) of AEs **2–10** are shown in Figure 5, and the total light emitted from each AE is shown in Figure 6.

Figure 5 indicates that all of the AEs show maximum emission levels in the millions of RLU at pH values from 10 to 12. For most compounds, the same is true at pH 9, but Compound **6** is an exception, with a maximum RLU emission level at pH 9 in the hundreds of thousands rather than millions. This trend is even clearer at pH 8, at which Compounds **2**, **3**, and **6** all show maximum RLU values in the hundreds of thousands, while at pH 7, none of the compounds reaches a million RLUs. Indeed, the three lowest level emitters at pH 7 (again Compounds **2**, **3**, and **6**) show maximum emission only in the tens of thousands of RLUs or lower, while all of the other compounds emit in the hundreds of thousands. This trend clearly does not correlate with the pKa values of the corresponding phenols (see Figure 4), which would predict that Compounds **2** and **10** would be at one end of the range and Compounds **8** and **9** at the other end of the range. This probably reflects the direct interaction between the OH group and the *ortho*-substituent in the phenol through factors such as intramolecular hydrogen bonding or geometrical constraints, which may affect the ease of ionization of the phenol in some of the cases. There is a somewhat better, albeit qualitative, correlation with Hammett σ_p values [32, 33] in that compounds having the substituents with the three lowest σ_p values result in the three lowest emission maxima at low pH values. It is not unreasonable that the compounds with less electron-withdrawing substituents would undergo slower reactions than those with more strongly electron-withdrawing substituents, which would lead to a later and lower emission maximum value, as observed particularly at pH 7.

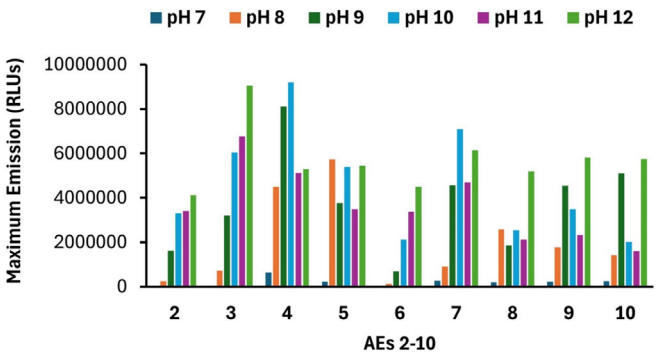

FIGURE 5 Maximum intensity of emission (relative light units [RLUs]) from acridinium esters (AEs) **2–10** at pH 7–12.

The trends for total emission values are shown in Figure 6. In all cases, the total emission, and therefore the relative chemiluminescent yield, increases from pH 7 but reaches a peak between pH 8 and 10 before decreasing as the pH level increases further. It would be expected that the rate of the chemiluminescent reaction would increase as the pH of the reaction medium increases. If the acquisition time for light collection would be insufficient for the reaction to go to completion at the lower pH values, this could explain why the quantum yield would increase as the pH increases at the lower pH values. However, that alone should not lead to a reduction in the chemiluminescent quantum yield at the higher pH values. The reduction in quantum yield at higher pH values suggests that a competing reaction is becoming more successful in competing with the chemiluminescent reaction under such conditions. Possible competing reactions could be the formation of a pseudo base (addition of hydroxide ion to the 9-position of the acridinium ring) at higher pH or hydrolysis of the ester group. It should be noted that steric hindrance from the ortho-substituent could affect the formation of the pseudo base, ester hydrolysis, and the chemiluminescent reaction to different extents.

For most of the AEs, the maximum chemiluminescent quantum yield occurs at or close to pH 8, but for Compounds **2**, **3**, and **6**, the peak occurs at around pH 9–10. Again, there is no good correlation between the pKa values of the corresponding phenols and either the RLU total emission value or the pH at which the maximum total emission value occurs for the AEs. A rough qualitative correlation with substituent σ_p values is observed for the pH at which the maximum quantum yield occurs, with the compounds containing the substituents having the three lowest σ_p values exhibiting the maximum at higher pH levels than the other AEs. However, the maximum quantum yields do not seem to relate in any predictable way to any obvious parameters.

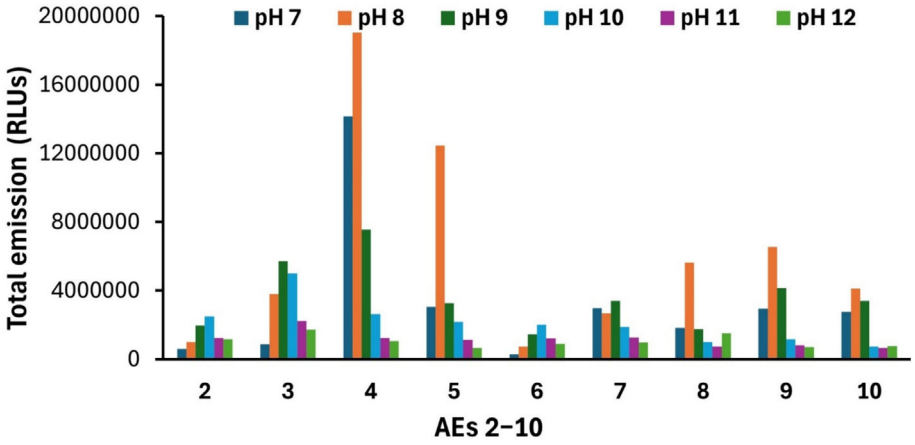

FIGURE 6 Total emission (relative light units [RLUs]) from acridinium esters (AEs) **2–10** at pH 7–12.

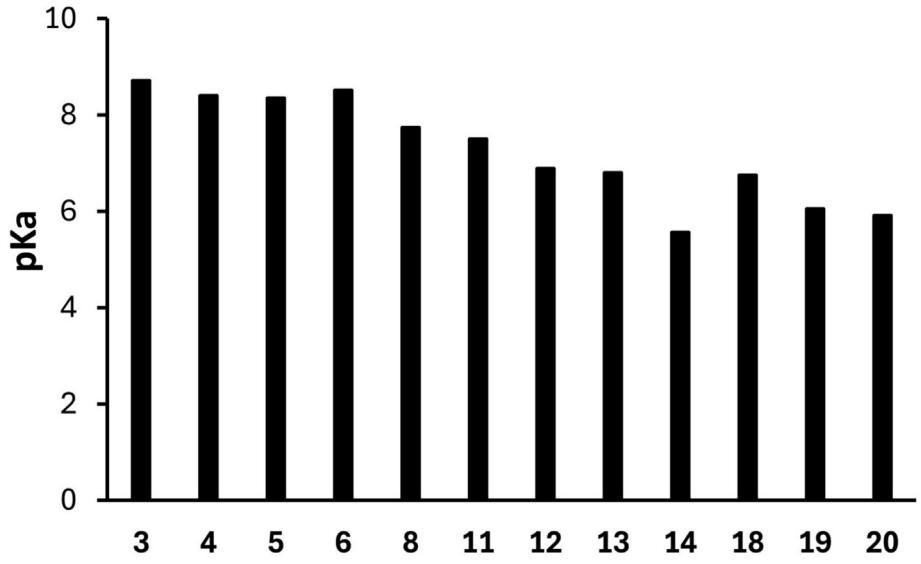

FIGURE 7 The pKa of the phenols associated with the ester groups of acridinium esters (AEs) **3–6**, **8**, **11–14**, and **18–20**.

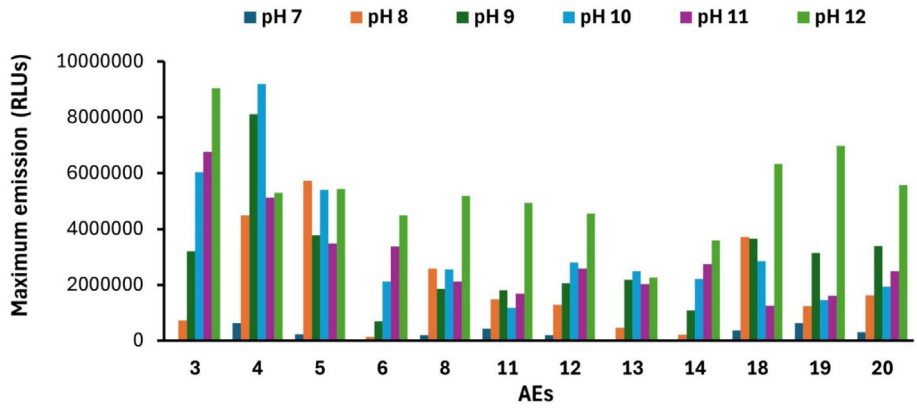

FIGURE 8 Maximum intensity of emission (relative light units [RLUs]) from acridinium esters (AEs) **3–6**, **8**, **11–14**, and **18–20**.

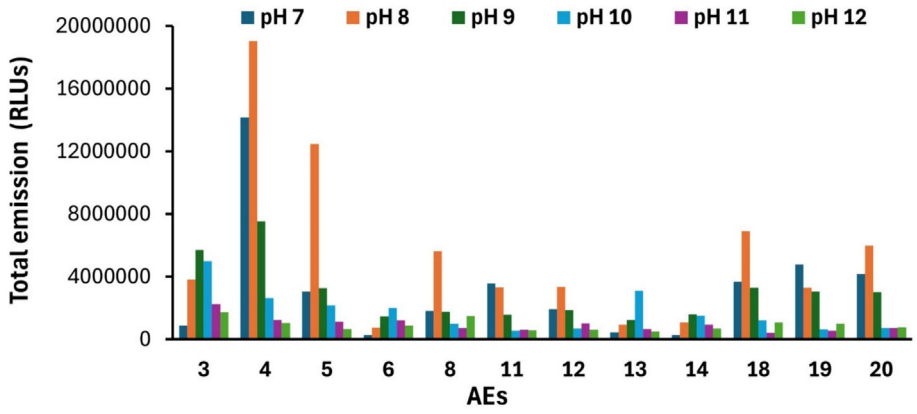

FIGURE 9 Total emission (relative light units [RLUs]) from acridinium esters (AEs) **3–6**, **8**, **11–14**, and **18–20**.

The most useful information from this series of experiments is that of the compounds studied, Compound **4**, the 2-chlorophenyl ester, offers the highest chemiluminescent quantum yield at pH 7–9.

The second group to be compared included 12 AEs that contain only identical halogen or CF_3 groups at the 2-, 2,6-, or 2,4,6-positions of the phenolic unit (i.e., AEs **3–6**, **8**, **11–14**, and **18–20**). The pKa of the phenols associated with the ester groups of AEs **3–6**, **8**, **11–14**, and **18–20** are shown in Figure 7 [30, 31].

The effects of pH (7–12) on the maximum chemiluminescent emission intensity and the total light emitted from each AE are shown in Figures 8 and 9, respectively. The trends represented in Figures 8 and 9 were similar to those depicted in Figures 5 and 6 for AEs **2–10**

in that all of the AEs provided substantial maximum emission levels at higher pH values. However, more significant differences were seen between AEs at the lower pH values, while the total emission levels of all the AEs except **19** (which peaks at pH 7) go through a maximum value at an intermediate pH value.

When looking at the detailed differences between these AEs, it must be remembered that there are various substitution patterns (mono-, di-, and tri-substituted phenolic units), as well as a variety of substituents (bromo, chloro, fluoro, iodo, and trifluoromethyl substituents). The AEs with two identical substituents in the 2- and 6-positions of the phenolic component (i.e., Compounds **11–14**) showed lower maximum and total emissions at almost every pH value than their corresponding 2-substituted (Compounds **3**, **4**, **5**, and **8**) or 2,4,6-tri-substituted derivatives (**18–20**). The results for the mono- and tri-substituted derivatives were somewhat similar to each other. However, there was a small reduction in the values for the tri-substituted compounds compared with the mono-substituted compounds under many pH conditions. Increasing substitution within this series of compounds always leads to a decrease in the pKa values of the corresponding phenols (Figure 7), which would be expected to increase the chemiluminescent rate and yield if that were the main influence on the reactions of the AEs. However, the additional *ortho*-substituents also cause increased steric hindrance, which hinders the hydroperoxide anion from attacking and would be expected to lead to a decrease in the rate and yield of chemiluminescence. Such steric hindrance seems to have had a more significant effect than pKa in the case of the disubstituted derivatives, as these show lower chemiluminescent yields and maximum intensities than the corresponding mono-substituted ones. However, because the disubstituted and tri-substituted phenols have the same degree of steric hindrance, the further decrease in pKa with the third substitution leads to an increase in yield and maximum intensity of the emission.

The final group of miscellaneous AEs (**15–17** and **21–25**) differs in both the nature and positions of the substituents, so trends are more difficult to discern. However, the effect on pKa (Figure 10) seems to be greatest for compounds containing a nitro group, regardless of its position. In contrast, an *ortho*-trifluoromethyl group has more effect than an *ortho*-acyl group on the pKa of the phenols associated with these AEs. The effects of pH (7–12) on the maximum chemiluminescent emission intensity and the total light emitted from AEs **15–17** and **21–25** are shown in Figures 11 and 12, respectively.

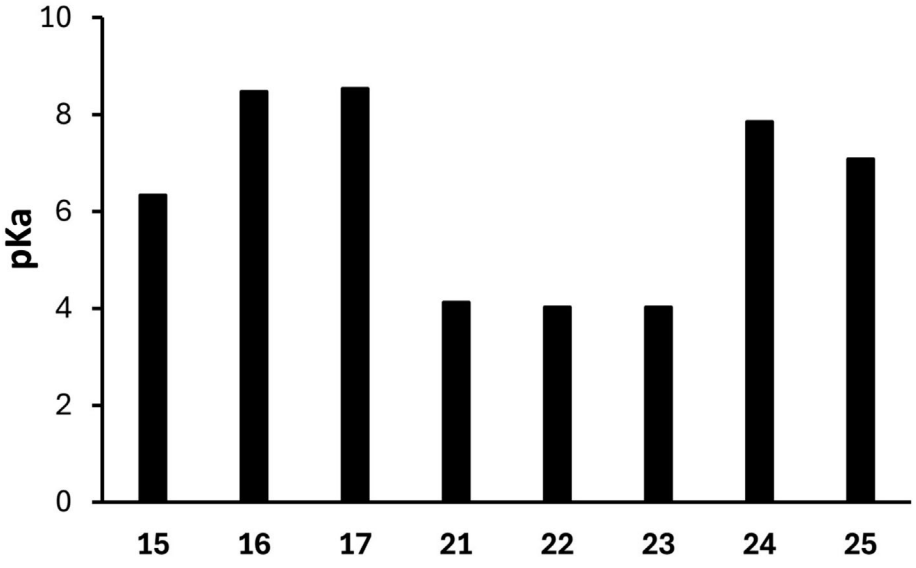

FIGURE 10 The pKa of the phenols associated with the ester groups of acridinium esters (AEs) **15–17** and **21–25**.

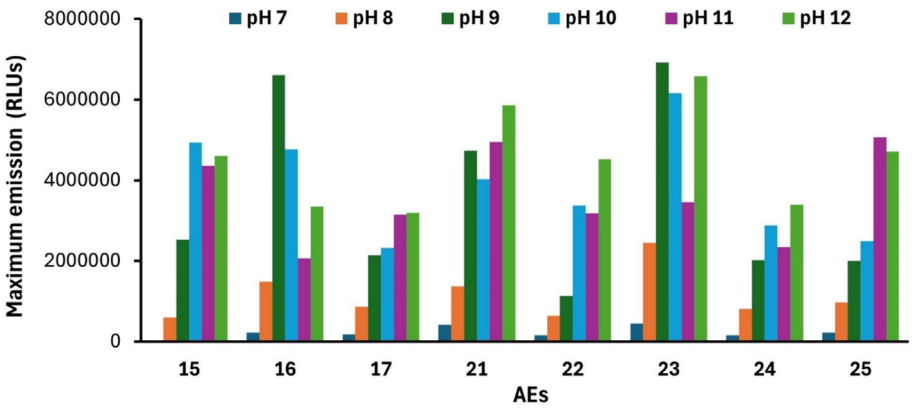

FIGURE 11 Maximum intensity of emission (relative light units [RLUs]) from acridinium esters (AEs) **15–17** and **21–25**.

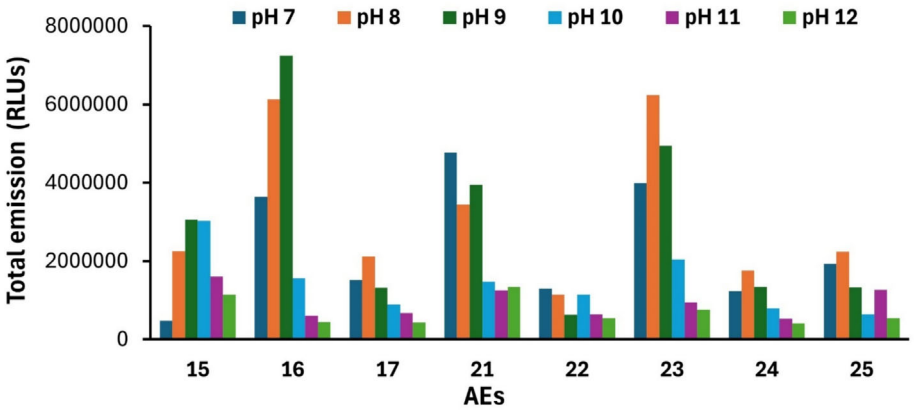

FIGURE 12 Total emission (relative light units [RLUs]) from acridinium esters (AEs) **15–17** and **21–25**.

AE **15** contains iodo and CF_3 groups at the *ortho*-positions of the aryloxy moiety and can therefore be compared with **6** (2-iodophenol), **8** (2-trifluoromethylphenol), and **14** (2,6-bis(trifluoromethyl)phenol). The differences in chemiluminescent behavior are most marked for maximum emission values at low pH (pH 7 and 8). A single iodo group (Compound **6**) results in a much greater drop in maximum emission value, compared with the simple phenyl AE (**2**), than a single CF_3 group (Compound **8**), but when two *ortho*-CF_3 groups are present (Compound **14**), the effect is similar to when just a single iodo group is present. Replacing one of the CF_3 groups of **14** by I (Compound **15**), however, has relatively little additional effect. It would appear that at the low pH values, the presence of either a single polarisable iodo group or two bulky groups (I or CF_3) lowers the maximum emission value to such an extent that emission is at a very low level. The reactions are slower than for most other AEs, which would cause the reactions to be incomplete at the end of the measuring period for total emission and also permit time for any non-emissive side reactions to gain prominence, both of which factors should lead to a decrease in the recorded total emission values. Indeed, this is the case, and all three of the thus-affected compounds (**6**, **14**, and **15**) show very low total emission at pH 7. The profiles for the total emission of these three compounds are actually very similar across the range of pH values.

The AEs **16** and **17** can loosely be compared with Compounds **9** and **10** but with a bulkier acyl group in the *ortho*-position and an additional halogen substituent at the *para*-position, where it would not further influence the steric interactions. Compounds **24** and **25** can be compared with compound **10**, but with two additional halogen substituents in the 4- and 6-positions, or with Compounds **19** and **20**, with one of the *ortho*-halogen substituents replaced by an acetyl group. All four compounds (**16**, **17**, **24**, and **25**), along with Compound **10**, contain an *ortho*-acyl group, and all except **10** contain at least one additional halogen substituent. In terms of the total emission levels, all of the compounds containing an *ortho*-acyl group, and even the trihalogen-compounds **19** and **20**, show qualitatively similar pH profiles, with a maximum at low pH (7–9) and tailing off substantially at higher pH (10–12). However, AE **16** shows a greater total emission value than the rest at the lower end of the pH range. The maximum intensities for the ortho-acyl compounds are again qualitatively similar, with the maximum value rising as the pH rises. However, AE **16** again shows a somewhat different pattern, with the maximum level occurring at a lower pH range (9–10) and then falling again when the pH increases further. It is not clear why **16** behaves somewhat differently than the other acyl derivatives.

AEs **21** (4,6-dichloro-2-nitrophenoxy derivative) and **24** (2-acetyl-2,4-dichlorophenoxy derivative) are similar to **19** (2,4,6-trichlorophenoxy derivative) except for one substituent, *ortho*-nitro or *ortho*-acetyl, respectively. AE **25** has a similar relationship to **20** as **24** does to **19**, while **23** has a *para*-nitro group instead of the bromo-substituent in **20**. AE **22** has not only an *ortho*-nitro substituent but also an *ortho*-fluoro substituent, so it is not just a simple substitution of one group in comparison to **20**. The maximum emissions of AEs **19–25** did not show any meaningful trends, although there were some differences. The total emission from **19** was significantly higher than that of **24** but lower than that of **21** at most pH values. The same trend was noticed with **20** and **25** as with **19** and **24**, although the difference was less significant. Because a similar trend was seen with AEs **4** and **5** in comparison to **10**, it is reasonable to conclude that the replacement of an *ortho*-halogen substituent by an *ortho*-acetyl substituent causes a lowering of total emission at most pH values. Because the σ_p value of the acetyl group (0.50) is larger than that of Cl (0.23) or Br (0.23), suggesting that the electron-withdrawing tendency of the acetyl group at the *ortho*-position would also be greater than that of Cl or Br at the *ortho*-position, it is likely that the lower total emission results from the increased steric interactions with the acetyl group.

The σ_p value of the nitro group (0.78) is significantly greater than that of any of the other substituents present in the compounds under investigation in this section. The pKa values of all of the nitro-group-containing phenols corresponding to Compounds **21–23** were significantly lower than the related phenols without a nitro group, regardless of the position of the nitro group or the nature of the other substituents. It, therefore, would not be too surprising for the nitro compounds to show an increase in emission yield because of faster and more complete reactions within the light-collection period. This was the case for AEs **21** and **23**, but not for AE **22**, or indeed for the mono-substituted nitro Compound **7** in comparison with the other mono-substituted AEs (**3–6**).

3.2.2 | Chemiluminescent stability

The stabilities of the various AEs were investigated in buffers of different pH values (6, 7, and 8) at different temperatures (4, 25, and 37°C). These conditions were chosen as representative of the sorts of conditions that might be used in the storage of biological samples or during hybridizations with probe molecules containing AEs of these types. A small sample of each AE solution was removed at various time intervals, and the total chemiluminescence emitted was measured under normal luminometer conditions over 15 s. The drop in the total light emission was used as an indication of the stability of the AE in the conditions described. As an example, the drop in chemiluminescence of **21** is shown in Figure 13. Note that for this AE, because of the slowness of the decay in such conditions, the pH 6, 4°C incubation was monitored over 200 h, while the room temperature and 37°C incubations at pH 7 and 8 required monitoring only for 25 h. The remaining incubations were monitored for 100 h. As can be seen from this example, AE **21** was more stable in lower pH buffers and at lower temperatures, as expected. This was, for the most part, the case for all of the AEs, but the rates of decay differed considerably for the individual cases.

In order to compare the relative stabilities of the different AEs in the different conditions, from graphs similar to those in Figure 13 for all the AEs, the times taken for the chemiluminescence outputs to diminish to 50% of their original values were recorded. These values for AEs **2–25** are represented in Figures 14, 15, and 16 using the same groupings as previously considered during the discussion of their chemiluminescence characteristics (see Figures 5, 8, and 11).

As can be seen by the comparison of Figure 14 with Figure 4, there is no strong correlation between the stability of the AEs in solution and the pKa values of the corresponding phenols. However, the AEs (**2**, **3**, **10**) corresponding to the three phenols with the highest pKa values do show less variation in the time for the chemiluminescent output to diminish to 50% of its original value under different conditions than is the case for the other AEs. The two AEs (**7**, **9**) corresponding to the phenols with the lowest pKa values show the lowest stability under higher temperature and pH conditions. However, AEs **6** and **8** are more stable at lower temperatures than would be

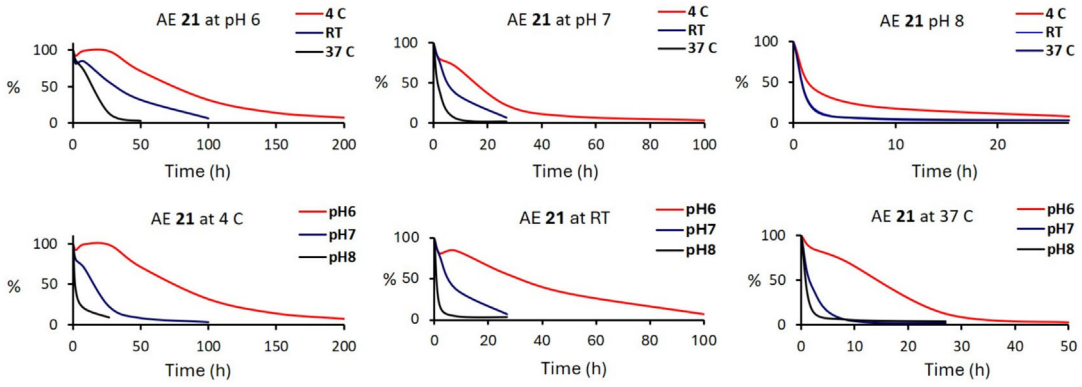

FIGURE 13 The stability of acridinium ester (AE) **21** at different pH values and temperatures. The plot is of the total light emitted as a percentage of the initial one against time in hours. RT, room temperature.

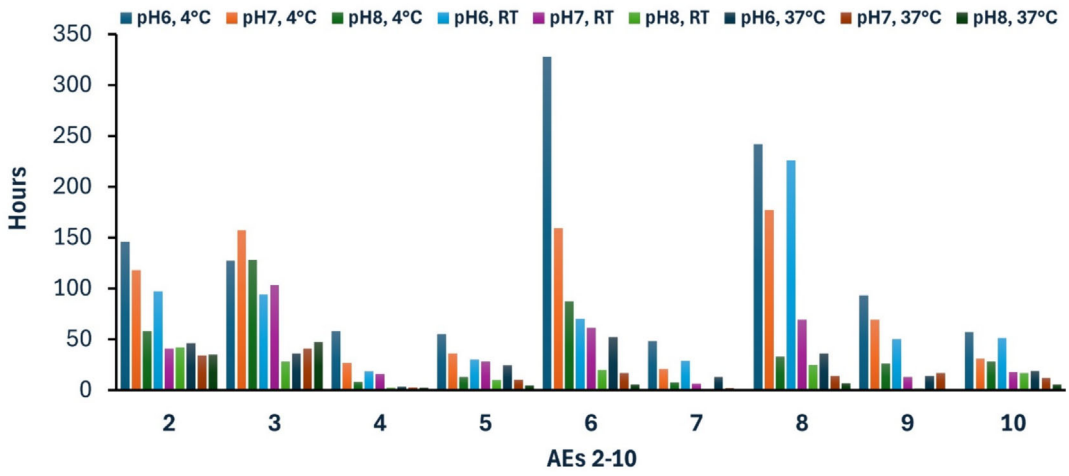

FIGURE 14 The time taken for the chemiluminescence output to diminish to 50% of its original value for acridinium esters (AEs) **2–10** at different pH values and temperatures. RT, room temperature.

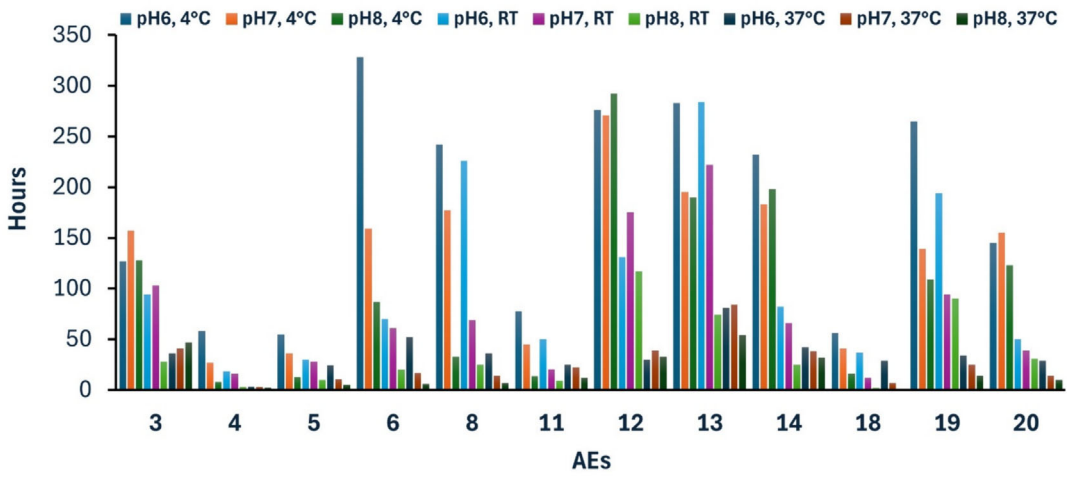

FIGURE 15 The time taken for the chemiluminescence output to diminish to 50% of its original value for acridinium esters (AEs) **3–6**, **8**, **11–14**, and **18–20** at different pH values and temperatures. RT, room temperature.

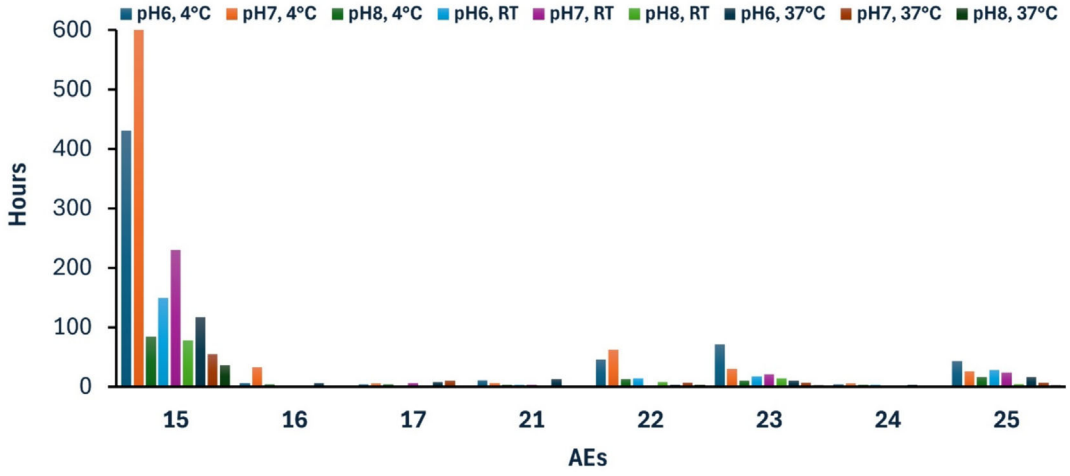

FIGURE 16 The time taken for the chemiluminescence output to diminish to 50% of its original value for acridinium esters (AEs) **15–17** and **21–25** at different pH values and temperatures. RT, room temperature.

expected on the basis of their pKa values in comparison to some of the other AEs. The lack of a definitive correlation between the stability of the AEs and the pKa of their corresponding phenols probably results primarily from two factors: (1) hydrogen bonding of some of the substituents with the phenolic OH group, which affects the pKa of the phenols; and (2) hindrance to attack at both the ester group and the 9 position of the AE unit by some of the substituents. The bulkier substituents would be expected to increase the stability of the AEs by direct shielding of the ester group from attack and also to cause a conformation change to disrupt the conjugation between the acridine unit and the carbonyl group (Figure 17). For example, the bulky trifluoromethyl group in **8** provides higher stability under lower temperature conditions than the unsubstituted AE **2** or the mono-halogen substituted AEs **3–5**, all of which have higher pKa values for the corresponding phenols. Similarly, an iodo group provides more hindrance than the other halogen groups, which could explain the higher-than-expected stability of **6** at lower temperatures.

FIGURE 17 Calculated structure for bis(trifluoromethyl)phenyl acridine-9-carboxylate, illustrating how the bulky trifluoromethyl groups force the carbonyl group out of the acridine plane.

By comparison of Figure 15 with Figure 7, it is again apparent that there is no good correlation between the stability of the AEs and the pKa values of the corresponding phenols. There are, however, other correlations that can be made for some sub-sets of the compounds. For example, with two Cl, Br, or CF_3 substituents at the 2- and 6-positions of the phenoxy unit, the AEs (**12–14**) are significantly more stable under most conditions than those (**4**, **5**, and **8**) with only one such substituent at the 2-position, presumably because of the increased hindrance commensurate with the additional substituent. However, this is not the case for the 2,6-difluoro AE **11** in comparison with the 2-fluoro AE **3**, presumably because the F group is not very bulky, and the electronic influence becomes dominant. Similarly, AEs **18–20**, which are related to AEs **11–13** by having a third F, Cl, or Br group, respectively, at the 4-position of the phenoxy unit, where there is no additional steric influence, were somewhat less stable because of the electronic influence of the additional substituent, as reflected in the pKa values of the corresponding phenols.

Among the group of AEs with mixed substituents (Figure 16), it is again clear that there is no good correlation with the pKa values of the corresponding phenols (Figure 10). The stability of AE **15** (containing trifluoromethyl and iodo substituents) should be compared with the stability of **6**, **8**, and **14**, which contain iodo, trifluoromethyl, and bis(trifluoromethyl) substituents, respectively. AEs **6** and **8** have one of the two *ortho* groups that **15** has, and **14** is similar to **15**, except that an iodo group replaces one trifluoromethyl group. Both **6** and **8** were already fairly stable, and **14** was more stable than **8**. Therefore, it would be expected that the stability of **15** would be broadly comparable to that of **14**, and this is the case.

Compounds **21** and **24** are similar to **19** (the trichloro derivative), except that one chloride has been substituted for an *ortho*-NO_2 or an *ortho*-COMe group, respectively. It is not surprising that such electron-withdrawing groups would reduce the stability of the AEs under all conditions. However, the extent of the destabilization was surprising (the chemiluminescence dropped to below 50% within around 10 h, even under the mildest conditions) in view of the steric bulk of the nitro and acetyl groups.

The AEs **20**, **23**, and **25** containing bromine (2,4,6-tribromo, 2,6-dibromo-4-nitro, and 2-acetyl-4,6-dibromo substituents, respectively) showed a similar pattern. AE **20** was more stable than the other two AEs. However, the reduction in stability was not as great as for the Cl compounds **21** and **24**, presumably because the two *ortho*-substituted bromine atoms provide greater steric hindrance.

The bulky benzoyl substituents at the *ortho*-position of the phenoxy ring in **16** and **17** did not improve the stability of the esters compared with the mono-substituted acetyl Compound **10**, which is probably because of the effect of the halogen substituents in the 4-position, which also reduce the pKa values of the corresponding phenols relative to that of **10**.

Comparing **22** with **3** and **7**, each of which has one of the two *ortho* groups on the phenoxy group of **22**, reveals that the stability of **7** is roughly comparable to that of **22**, despite the additional 2-fluoro and 4-bromo substituents, while **3** is considerably more stable. Evidently, the lack of stability of **22** is primarily determined by the effect of the nitro group, and the difference in pK_a between the phenols corresponding to **7** and **22** is compensated by the extra steric hindrance in **22**.

4 | CONCLUSIONS

Various AEs with electron-withdrawing substituents attached at the 2, 4, and/or 6-positions of the phenoxy unit have been synthesized, and their chemiluminescent properties and stabilities have been evaluated at different temperatures and in buffers of different pH values. The previously suggested correlation between the chemiluminescent properties of AEs and the pKa values of their associated phenols generally does not hold for such *ortho*-substituted phenyl esters. The steric effects of such substituents, as well as their electron-withdrawing natures, seem to play an important role in determining the properties. As would be expected, the average time taken for complete chemiluminescent emission from the AEs diminishes with increasing temperature and/or increasing pH of the triggering solution. However, within that average, the individual AEs show significant variation in both the time taken for the chemiluminescent reaction to go to completion and the total amount of light emitted (within a 15-s collection period). For example, the amount of light emitted from the 2-chlorophenyl ester (**4**) at pH 8 was more than 10 times greater than that emitted from the 2,6-bis(trifluoromethyl) phenyl ester (**14**). The latter reaction is presumably slowed down considerably by the two bulky trifluoromethyl groups, which could result in some light not being emitted within the collection period, as well as allowing time for non-radiative pathways to compete with emissive pathways.

The substitution pattern of the phenoxy unit also influences the rate of decomposition of the AEs in buffers of different pH values, as determined by the time taken for the amount of light emitted to diminish to half its original value. In general, when two identical substituents are present in the 2- and 6-positions, the compound is significantly more stable than when only a single substituent is present at the 2-position, despite the presence of the second electron-withdrawing group. This presumably arises because of greater steric hindrance resulting from the presence of the second group. The exception is the 2,6-difluorophenyl ester (**11**), which is less stable than the 2-fluorophenyl ester (**3**), presumably because the fluoro group is too small to cause a significant steric effect but can still affect the rate of reaction by its electron-withdrawing tendency. The latter reasoning also applies to the addition of a third electron-withdrawing substituent at the 4-position, where it has no steric influence but does still have an electronic influence. Consequently, typically, 2,4,6-trisubstituted phenyl esters are more susceptible to decomposition than their disubstituted analogs. The presence of a nitro group had a significant destabilizing effect on all of the AEs in which it was present, regardless of the position of the group.

AE **4** (the 4-chlorophenoxy derivative) showed the greatest chemiluminescent yield, while AE **15** (the 2-iodo-6-(trifluoromethyl} phenoxy derivative) showed the greatest stability in low pH buffers.

AUTHOR CONTRIBUTIONS

Keith Smith: Conceptualization; data curation; supervision; formal analysis; methodology; project administration; resources; writing—review and editing; writing—original draft; validation; visualization; funding acquisition. **Andy M. Holland:** Data curation; investigation; formal analysis; validation; writing—review and editing; writing—original draft. **J. Stuart Woodhead:** Conceptualization; data curation; resources; writing—review and editing. **Gamal A. El-Hiti:** Data curation; formal analysis; visualization; validation; writing—review and editing; writing—original draft.

ACKNOWLEDGMENTS

We thank Molecular Light Technology Research Limited, Cardiff, UK, for funding and Cardiff and Swansea Universities for general support. G.A. El-Hiti acknowledges the support from the Researchers Supporting Project (number RSP2024R404), King Saud University, Riyadh, Saudi Arabia. We also thank Dr Mark C Elliott of Cardiff University for calculating the structure shown in Figure 17.

CONFLICT OF INTEREST STATEMENT

There is no conflict of interest to declare.

DATA AVAILABILITY STATEMENT

The data that support the findings of this study are available in the Supporting information of this article.

ORCID

Keith Smith https://orcid.org/0000-0003-4838-5651
Gamal A. El-Hiti https://orcid.org/0000-0001-6675-3126

REFERENCES

[1] L. Cinquanta, D. E. Fontana, N. Bizzaro, *Auto. Immun. Highlights* **2017**, *8*, 9.
[2] C. Dodeigne, L. Thunus, R. Lejeune, *Talanta* **2000**, *51*, 415.
[3] I. Weeks, *Chemiluminescence Immunoassay. Comprehensive Analytical Chemistry*, Vol. 29, Elsevier, Amsterdam **1992**.
[4] M. Nakazono, Y. Oshikawa, M. Nakamura, H. Kubota, S. Nanbu, *J. Org. Chem.* **2017**, *82*, 2450.
[5] T. Ma, M. Zhang, Y. Wan, Y. Cui, L. Ma, *Micromachines* **2017**, *8*, 149.
[6] L. Holec-Gąsior, B. Ferra, J. Czechowska, I. E. Serdiuk, K. Krzymiński, *Diagn. Microbiol. Infect. Dis.* **2018**, *91*, 13.
[7] M. Nakazono, S. Nanbu, T. Akita, K. Hamase, *J. Oleo Sci.* **2021**, *70*, 1677.
[8] I. Weeks, I. Beheshti, F. McCapra, A. K. Campbell, J. S. Woodhead, *Clin. Chem.* **1983**, *29*, 1474.
[9] S. Batmanghelich, J. S. Woodhead, K. Smith, I. Weeks, *J. Photochem. Photobiol. A* **1991**, *56*, 249.
[10] S. Batmanghelich, R. C. Brown, J. S. Woodhead, K. Smith, I. Weeks, *J. Photochem. Photobiol. B: Biol.* **1992**, *12*, 193.
[11] A. Natrajan, D. Sharpe, *Synth. Tetrahedron Lett.* **1996**, *37*, 8519.
[12] K. Smith, Z. Li, J. Yang, I. Weeks, J. S. Woodhead, *J. Photochem. Photobiol. A* **2000**, *132*, 181.
[13] K. Smith, J.-J. Yang, Z. Li, I. Weeks, J. S. Woodhead, *J. Photochem. Photobiol. A* **2009**, *203*, 72.
[14] A. Natrajan, D. Sharpe, *Org. Biomol. Chem.* **2013**, *11*, 1026.
[15] S. Wang, A. Natrajan, *RSC Adv.* **2015**, *5*, 19989.
[16] A. Natrajan, D. Wen, *Org. Biomol. Chem.* **2015**, *13*, 2622.
[17] B. Zadykowicz, J. Czechowska, A. Ożóg, A. Renkevich, K. Krzymiński, *Org. Biomol. Chem.* **2016**, *14*, 652.
[18] K. Smith, X. Mu, Z. Li, J. S. Woodhead, G. A. El-Hiti, *Luminescence* **2022**, *37*, 1982.
[19] K. Smith, X. Mu, Z. Li, A. M. Holland, J. S. Woodhead, G. A. El-Hiti, *Luminescence* **2023**, *38*, 487.
[20] K. Smith, X. Mu, Z. Li, J. S. Woodhead, G. A. El-Hiti, *Luminescence* **2023**, *38*, 1857.
[21] R. C. Brown, Z. Li, A. J. Rutter, X. Mu, O. H. Weeks, K. Smith, I. Weeks, *Org. Biomol. Chem.* **2009**, *7*, 386.
[22] K. A. Browne, D. D. Deheyn, G. A. El-Hiti, K. Smith, I. Weeks, *J. Am. Chem. Soc.* **2011**, *133*, 14637.
[23] A. Natrajan, D. Wen, *RSC Adv.* **2014**, *4*, 21852.
[24] A. Natrajan, D. Wen, D. Sharpe, *Org. Biomol. Chem.* **2014**, *12*, 3887.
[25] K. Smith, Z. Ahmed, J. S. Woodhead, G. A. El-Hiti, *J. Oleo Sci.* **2023**, *72*, 447.
[26] F. McCapra, *Proc. R. Soc. B: Biol. Sci.* **1982**, *215*, 247.
[27] F. McCapra, *Pure Appl. Chem.* **1970**, *24*, 611.
[28] K. Krzymiński, A. Ożóg, P. Malecha, A. D. Roshal, A. Wróblewska, B. Zadykowicz, J. Błażejowski, *J. Org. Chem.* **2011**, *76*, 1072.
[29] K. Krzymiński, P. Malecha, B. Zadykowicz, A. Wróblewska, J. Błażejowski, *Spectrochim. Acta A Mol. Biomol.* **2011**, *78*, 401.
[30] D. D. Perrin, B. Dempsey, E. P. Serjeant, *pKa prediction for organic acids and bases*, Springer, Dordrecht **1981**.
[31] M. D. Liptak, K. C. Gross, P. G. Seybold, S. Feldgus, G. C. Shields, *J. Am. Chem. Soc.* **2002**, *124*, 6421.
[32] D. H. McDaniel, H. C. Brown, *J. Org. Chem.* **1958**, *23*, 420.
[33] M. Charton, *Can. J. Chem.* **1960**, *38*, 2493.

SUPPORTING INFORMATION

Additional supporting information can be found online in the Supporting Information section at the end of this article.

How to cite this article: K. Smith, A. M. Holland, J. S. Woodhead, G. A. El-Hiti, *Luminescence* **2024**, *39*(6), e4794. https://doi.org/10.1002/bio.4794